Sustainable Food Technology

ROYAL SOCIETY OF CHEMISTRY

PAPER

View Article Online
View Journal | View Issue

Cite this: *Sustainable Food Technol.*, 2025, **3**, 822

A novel concoction method of Chinese medicinal and edible plants: probiotic fermentation, sensory and functional composition analysis†

Zhengxu An,‡[ab] Tong Ye,‡[bc] Junwei Yu,[d] Hongjun Wu,[e] Peirong Niu,[ab] Xiaobo Wei,[ab] Huiyan Liu*[ab] and Haitian Fang*[ab]

Probiotic fermentation is a novel concoction method of medicinal and edible plants with microbial-specific biotransformation function. Some dipeptides, nucleosides and flavonoids exhibit strong flavor and functional properties and play an important role in enhancing the sensory quality and functional composition, while probiotic fermentation may promote the increase of these substances and thus the quality of plants. In this study, *Lactobacillus paracasei* 5572 was used to ferment and concoct several Chinese medicinal and edible plants, including goji (*Lycium barbarum*), carrot, golden imperial chrysanthemum and inulin, and a product was developed by optimizing the ratio of these plants through sensory evaluation. The flavor and functional composition as well as the antioxidant activity of these plants were enhanced after fermentation concoction by determining total flavonoids and phenolics, assessing the effects on DPPH, ABTS and ·OH free radicals, and using metabolomics techniques, the molecular mechanism of which involved the probiotic increasing the content of the above compounds through 30 metabolic pathways. In conclusion, this study revealed that the probiotic fermentation method of concocting medicinal and edible plants could significantly enhance their sensory and functional qualities and also elucidated the molecular mechanisms involved, which might provide new ideas and insights for their sustainable development and research.

Received 16th March 2025
Accepted 3rd April 2025

DOI: 10.1039/d5fb00091b

rsc.li/susfoodtech

Sustainability spotlight

China possesses abundant resources of medicinal and edible plants (MEPs), but they are not fully utilized due to the complicated operation and poor taste of traditional concoction methods. Probiotic fermentation is a novel concoction method with microbial-specific biotransformation function, which can effectively improve the sensory and functional properties of MEPs. In recent years, consumers have increasingly demanded foods with both excellent taste and function to improve their health. Therefore, the fermentation of several popular MEPs into beverages by *Lactobacillus paracasei* 5572 not only reduces the waste of resources in traditional concoction methods and enables large-scale industrial production of MEPs, but also meets the demands of consumers and promotes the sustainable development of the functional food market.

1. Introduction

With the gradual enhancement of people's health awareness, the global research on medicinal and edible plants (MEPs) with natural and health-promoting properties has also gradually increased.[1] China possesses abundant resources of MEPs and has accumulated valuable experience in their processing and concoction from ancient times to the present.[2] Nowadays, probiotic fermentation as a new type of concoction method has become popular due to its dual ability to improve both the medicinal and edible qualities of MEPs.

Goji (*Lycium barbarum*) is a traditional MEP that have been proved to have high medicinal and edible properties due to its richness in bioactive compounds, with strong antioxidant, anti-fatigue, and immune-enhancing effects.[3] Carrot is a major source of natural β-carotene,[4] and probiotic-fermented carrot juice has a positive effect on the regulation of blood glucose, oxidative stress, and lipid metabolism.[5] Golden imperial chrysanthemum is rich in flavonoids, and its solubility and antioxidant activity can be further improved after being crushed.[6] Inulin is a natural

[a]*School of Food Science and Engineering, Ningxia University, Yinchuan 750021, Ningxia, China. E-mail: liuhy@nxu.edu.cn; fanght@nxu.edu.cn; Tel: +86 13709591521; +86 13895419445*

[b]*Ningxia Key Laboratory for Food Microbial-Applications Technology and Safety Control, Ningxia University, Yinchuan 750021, Ningxia, China*

[c]*School of Life Sciences, Ningxia University, Yinchuan 750021, Ningxia, China*

[d]*Ningxia Zhongning Goji Industry Innovation Research Institute, Zhongwei 755100, Ningxia, China*

[e]*Ningxia Xiajin Dairy Group Co., Ltd, Wuzhong 751100, Ningxia, China*

† Electronic supplementary information (ESI) available. See DOI: https://doi.org/10.1039/d5fb00091b

‡ These authors contributed equally to this work.

polysaccharide with strong anti-inflammatory, antioxidant, intestinal flora regulating and immune-enhancing abilities and has a wide range of applications in drug delivery, prebiotics and disease treatment.[7,8] By mixing these Chinese MEPs and concocting them using probiotic fermentation, their sensory quality and functional composition are expected to be enhanced.

In previous studies, *Lactobacillus paracasei* has been widely used due to its potent environmental tolerance and rich probiotic functions.[9,10] Marnpae *et al.*[11] utilized *L.paracasei* CASEI 431 in the fermentation of Gac juice, resulting in the enhancement of β-carotene, organic acids, antioxidant activity, and cholesterol-lowering efficacy. Similarly, Midlej *et al.*[12] demonstrated a significant increase in total phenolic content and stability of antioxidant activity after the fermentation of Araticum (*Annona crassiflora*) using *L.paracasei* LBC-81. However, there has been limited research on concocting Chinese MEPs such as *L.barbarum* fermented by *L.paracasei*, and the changes in their nutrient composition and antioxidant activity during fermentation also need to be further explored.

In the current technological landscape, metabolomics has emerged as a pivotal tool for elucidating changes in the nutritional composition of probiotic fermented foods. Chen *et al.*[13] employed metabolomics to analyze yoghurt fermented by *L.paracasei* ZFM54, and the findings underscored that fermentation augmented the concentration of volatile acids and diversified the array of untargeted metabolites, culminating in a pronounced enhancement of the yoghurt's flavor and functional attributes. Similarly, Xie *et al.*[14] leveraged both targeted and untargeted metabolomics methodologies to identify the metabolites present in *Lycium barbarum* Juice (LBJ) fermented by *Lactiplantibacillus plantarum*, and the results demonstrated that fermentation engendered the accumulation of a variety of functional and palatable compounds, such as lactic acid, γ-aminobutyric acid, phenylglycolide, and acetyl derivatives, thereby elevating the quality of the LBJ. Nevertheless, there remains a paucity of research examining the metabolomic changes that occur both before and after fermentation of composite LBJ by *L.paracasei*.

In this research, we developed a *L.barbarum* herbal mixed beverage fermented by *L.paracasei* 5572. After sensory evaluation, formulation optimization and the functional composition, antioxidant activity inspection of unfermented *L.barbarum* herbal mixed juice (UFMJ) and the fermented *L.barbarum* herbal mixed juice (FMJ), LC-MS/MS metabolomics was used to measure the non-volatile metabolic products in both. Furthermore, the pathways enriched with these metabolites were analyzed, aiming to gain a deeper understanding of the molecular mechanisms of the changes in the sensory quality and functional composition of the composite LBJ before and after fermentation and to provide a theoretical basis for the development and research of probiotic fermentation concoction of more Chinese MEPs.

2 Materials and methods

2.1 Fermentation concoction process

Fresh carrots (purchased from a local supermarket in Zhongwei, China) were washed and cut into pieces, and the juice was extracted at a ratio of 1 : 5 (carrot: water, m/v) and then filtered through an 80-mesh sieve. A single-factor test was conducted to make a preliminary determination of the formulation of the product. 15 combinations of Chinese MEP ingredients were made according to the ratios of 33%, 34%, 35%, 36% and 37% for the addition of LBJ (Ningxia Zhongning Goji Industry Innovation Research Institute, Zhongwei, China); 23%, 23.5%, 24%, 24.5% and 25% for the addition of carrot juice (CJ); and 1.8%, 1.9%, 2.0%, 2.1% and 2.2% for the addition of golden imperial chrysanthemum powder (GICP, Ningxia Zhongning Goji Industry Innovation Research Institute, Zhongwei, China). Next, 3% of inulin (Chongqing Joywin Natural Products Co., Ltd, Chongqing, China) was added to them to improve the flavor and enhance the function. To ensure proper consistency, 36% purified water was finally supplemented to make UFMJ, which was pasteurized (65 °C, 30 min), and then stored at 4 °C after cooling. *L.paracasei* 5572 (Ningxia Key Laboratory for Food Microbial-Applications Technology and Safety Control, Yinchuan, China) was pre-cultured for activation and its growth curve was determined, after which the bacterial suspension was inserted into the pasteurized UFMJ with 5% inoculum volume and fermented at 37 °C for 24 h to obtain FMJ, and the 15 FMJs from the single-factor test were subjected to sensory evaluation in order to select the excellent formulations of the product.

2.2 Formulation optimization of medicinal and edible plants

To further optimize the sensory quality of FMJ, the formulation of MEPs was modified by response surface methodology (RSM), which is a mathematical technique combining polynomial equations with the fitting of experimental data to construct statistical models to optimize individual factors as well as potential interactions between different factors. Box–Behnken Design (BBD) is suitable for the optimal extraction of process parameters and can evaluate interactions based on the results of single-factor tests.[15] In this experiment, the better level of each factor determined in the single-factor test was selected, and three factors, including LBJ addition (A), CJ addition (B) and GICP addition (C), were used as the response factors, and the sensory scores were used as the response values. The BBD test was performed using Design Expert 13 software to determine the product formulation with the optimal sensory quality (Table 1).

2.3 Sensory evaluation

This sensory evaluation was approved by our institution's Science and Technology Ethics Committee for ethical

Table 1 Factor levels for Box–Behnken design

		Factor levels		
Symbols	Response factors	−1	0	1
A	LBJ addition (%)	35	36	37
B	CJ addition (%)	24	24.5	25
C	GICP addition (%)	1.8	1.9	2.0

permission to conduct a human sensory evaluation study (Approval No. NXU-H-2023-160). 15 participants with more than two years of experience in food sensory evaluation were selected from the Ningxia Zhongning Goji Industry Innovation Research Institute, which is qualified to conduct sensory evaluation experiments. The participants included 8 males and 7 females, with an age distribution between 20 and 50 years old, and all of them were voluntarily enrolled and had signed the relevant informed consent in advance and were also guaranteed the right to withdraw from the evaluation at any time without having to give a reason. In addition, the products for this sensory evaluation were beverages within the food category, and their quality had been tested and complied with the national standard of the People's Republic of China (Standard No. GB 7101-2022) before the sensory evaluation to ensure that they were safe to drink.

This sensory evaluation was carried out according to Huang's method[16] with slight modifications, and the FMJ was evaluated on a 100-point scale in 4 aspects: color (20%), texture (20%), aroma (30%) and taste (30%), with higher scores indicating better performance on this indicator (for sensory evaluation scoring criteria, see the ESI and Table S1†). During the evaluation, the room temperature was maintained at 25 ± 1 °C, with sufficient light, no odors and no noise. The order of the samples in this evaluation was randomized and the participants were not known. The interval between samples was 3 min, and the mouth was rinsed with purified water.

2.4 Determination of functional composition and *in vitro* antioxidant activity

2.4.1 Total flavonoid content. The total flavonoid content was determined by the aluminum nitrate colorimetric method[17] with slight modifications. 1 ml of each sample (UFMJ and FMJ) was mixed with 5 mL of anhydrous ethanol and centrifuged at 10 000 rpm for 10 min. 0.1 mL supernatant was mixed with 0.3 mL of 5% $NaNO_2$ solution and then left to stand for 5 min. 0.3 mL of 10% $Al(NO_3)_3$ solution was added and reacted for 6 min, and after the reaction was completed, 2 mL of 1 M NaOH solution was added and mixed. The absorbance was measured at 510 nm after standing for 15 min at room temperature. In addition, the standard curve was drawn with rutin standard, and the total flavonoid content of the sample was calculated according to the standard curve. The results were expressed as rutin equivalents (mg mL^{-1}).

2.4.2 Total phenolic content. The total phenolic content was determined by the Folin–Ciocalteu staining method[18] with a slight modification. 1 mL of each sample (UFMJ, FMJ) was mixed with 5 mL 60% ethanol and centrifuged at 10 000 rpm for 10 min. 1 mL supernatant was mixed with 2.5 mL Folin–Ciocalteu reagent, 2.5 mL 15% Na_2CO_3 solution and 4 mL deionized water. The absorbance value was measured at 760 nm after standing for 2 h at room temperature. In addition, the standard curve was drawn with the gallic acid standard, and the total phenolic content in the sample was calculated according to the standard curve. The results were expressed as gallic acid equivalents (mg mL^{-1}).

2.4.3 DPPH radical scavenging activity. The 2,2-diphenyl-1-picrylhydrazyl (DPPH, Yuanye Biotech, Shanghai, China) radical scavenging rate was determined by referring to Yang's method[19] with slight modifications. In addition, Vc was used as a positive control for the free radical scavenging rate in this study because of its proven antioxidant mechanism.[20] 1 mL of each experimental sample (UFMJ and FMJ) and positive control sample (Vc) with different concentrations was mixed with 2 mL of 0.04 mg mL^{-1} DPPH ethanol solution, respectively. The absorbance value was measured at 517 nm after 30 min of reaction at room temperature and protected from light. The DPPH radical scavenging rate (%) was calculated according to eqn (1):

$$\text{DPPH radical scavenging rate (\%)} = 1 - \frac{A_1 - A_2}{A_0} \times 100\% \quad (1)$$

where A_0 represents H_2O mixed with DPPH ethanol solution; A_1 represents the sample solution mixed with DPPH ethanol solution; A_2 represents the sample solution mixed with anhydrous ethanol.

2.4.4 ABTS radical scavenging activity. The 2,2′-azinobis-(3-ethylbenzthiazoline-6-sulphonate) (ABTS, Yuanye Biotech, Shanghai, China) radical scavenging rate was determined using Wang's method[21] with slight modifications. 0.89 mL of 140 mmol L^{-1} $K_2S_2O_8$ solution was mixed with 50 mL of 7 mmol L^{-1} ABTS solution overnight to make the stock solution, which was diluted before the start of the experiment until its absorbance at 734 nm was 0.70 ± 0.02, and then 0.1 mL of each experimental sample (UFMJ and FMJ) and positive control sample (Vc) with different concentrations was mixed with 1.9 mL ABTS solution. The absorbance value was measured at 734 nm after 6 min of reaction at room temperature and protected from light. The scavenging rate (%) of ABTS radicals was calculated according to eqn (2):

$$\text{ABTS radical scavenging rate (\%)} = 1 - \frac{A_1 - A_2}{A_0} \times 100\% \quad (2)$$

where A_0 represents H_2O mixed with ABTS solution; A_1 represents the sample solution mixed with ABTS solution; A_2 represents the sample solution mixed with H_2O.

2.4.5 ·OH radical scavenging activity. The ·OH radical scavenging rate was determined by referring to Smirnoff's method[22] with slight modifications. 1 mL of each experimental sample (UFMJ and FMJ) and positive control sample (Vc) with different concentrations was mixed with 1 mL of 9 mmol L^{-1} $FeSO_4$ solution and 1 mL of 9 mmol L^{-1} H_2O_2 solution and left to stand for 11 min, and then 1 mL of 9 mmol L^{-1} salicylic acid ethanol solution was added and kept at 37 °C for 30 min. After cooling, the mixture was centrifuged at 900×*g* for 11 min and its supernatant was taken to measure the absorbance value at 510 nm. The ·OH radical scavenging rate (%) was calculated according to eqn (3):

$$\text{·OH radical scavenging rate (\%)} = 1 - \frac{A_1 - A_2}{A_0} \times 100\% \quad (3)$$

where A_1 represents the sample solution mixed with $FeSO_4$ solution, H_2O_2 solution and salicylic acid ethanol solution; A_0 represents H_2O instead of the sample solution; A_2 represents anhydrous ethanol instead of the salicylic acid ethanol solution.

2.5 Metabolomic analysis

In this study, a UPLC-ESI-Q-Orbitrap-MS system (UHPLC, Shimadzu Nexera X2 LC-30AD, Shimadzu, Japan) coupled with a Q-Exactive Plus (Thermo Scientific, San Jose, USA) was used for metabolomic analysis.

100 μL of samples (UFMJ and FMJ) were mixed with 400 μL of cold methanol-acetonitrile (1 : 1, v/v) and sonicated for 1 h at 250 W in an ice bath. Then, they were incubated at −20 °C for 1 h and centrifuged at 14 000×*g* for 20 min at 4 °C. For liquid chromatography, pre-processed UFMJ and FMJ samples were separated on an ACQUITY UPLC® HSS T3 column (2.1 × 100 mm, 1.8 μm) (Waters, Milford, MA, USA), respectively. The column flow rate was maintained at 0.3 mL min^{-1}, and the mobile phase A was 0.1% FA aqueous solution and B was 100% acetonitrile (ACN). Gradient elution was performed under the following conditions: buffer B was 0% for 2 min, rose linearly to 48% for 2-6 min, rose to 100% for 6–10 min and was maintained for 2 min, and then fell to 0% within 0.1 min before re-equilibrating for 3 min.

For mass spectrometry data collection, electrospray ionization (ESI†) was performed in positive and negative ion modes, and the conditions of the HESI source were as follows: spray voltages of 3.8 kV (positive) and 3.2 kV (negative); a capillary temperature of 320 °C; a sheath gas (nitrogen) flow rate of 30 arbitrary units (arb); an auxiliary gas flow rate of 5 arb; a probe heater temperature of 350 °C; the S-Lens RF level was 50. The MS acquisition range was *m*/*z* 70–1050 Da; the scan range was *m*/*z* 200 with a resolution of 70 000 and a maximum injection time of 100 ms; the MS/MS scan range was *m*/*z* 200 with a resolution of 17 500 and a maximum injection time of 50 ms. The MS2 separation window was 2 *m*/*z* and the normalized collision energies of the fragments (stepped) were 20, 30 and 40.

2.6 Statistical analysis

SPSS 23.0 (Chicago, IBM, USA) was used to perform analysis of variance (ANOVA) and LSD Fisher's test on the experimental data to distinguish significant differences between the samples ($P < 0.05$). OriginPro 2021 (OriginLab, Northampton, MA) was used to record standard curves and plots. All the above experiments were repeated three times, and the results were expressed as mean ± standard deviation.

3 Results

3.1 Determination of fermentation concoction time

The growth curve represents the population growth characteristics of microorganisms when cultured in liquid under specific environmental conditions. It provides an intuitive reflection of the growth characteristics of strains. As shown in Fig. 1A, *L.paracasei* 5572 exhibited no significant delay period in MRS liquid medium and rapidly entered the logarithmic growth phase with increasing culture time. At approximately 16 hours, the strain entered the stabilization period. During this time, the growth rate and physiological activity of the strain decreased, while its metabolites accumulated in large quantities within the fermentation system. The stabilization period of the strain ended and entered the decay period at approximately 24 h. The accumulation of metabolites ceased and reached its maximum value at this point. Therefore, 24 h was chosen as the fermentation concoction time for UFMJ.

3.2 Analysis of preliminary formulation

As shown in Fig. 1B–D, the sensory scores increased as the amount of the three Chinese MEP additions increased. However, when the additions of LBJ, CJ, and GICP exceeded 36%, 24.5%, and 1.9%, respectively, the sensory scores exhibited a decreasing trend. The optimal amount of LBJ for the beverage is 36% to avoid a shallow fruity flavor or excessive astringency. Similarly, the optimal amount of CJ is 24% to prevent the beverage from being too dark or bitter, and for GICP, an amount that is too low will result in a weak tea and floral flavor, while an amount that is too high will mask the aroma of other ingredients, so its optimal amount is 1.9%.

3.3 Analysis of formulation optimization

Based on the results of the single-factor test, a RSM optimization analysis was conducted with the BBD test. The ANOVA of the BBD test is shown in Table 2, and the detailed scheme and results are shown in ESI, Table S2.† The regression equation was obtained by fitting a regression to each factor using sensory scores as the response value. The equation is $Y = 92.96 + 0.32A + 0.70B - 0.62C - 0.64AB - 0.95AC + 0.56BC - 1.32\,A^2 - 1.61B^2 - 1.59C^2$. Table 2 shows that the model had a *P*-value of less than 0.01, indicating high significance. The misfit term had a *P*-value greater than 0.05, indicating the absence of a misfit phenomenon, so the model was meaningful and could be used to speculate on the test results. The R^2 value for this model was 0.9802, indicating that it adequately explains 98.02% of the variation in sensory ratings. The ${R_{adj}}^2$ was 0.9548, which is not significantly different from the original R^2 of the model. Additionally, the value of C.V. was 0.40 and the value of Adeq Precision was 18.086, indicating that the test was conducted accurately and reliably. The ANOVA results indicated that primary items B and C, interaction item AC, and secondary items A^2, B^2, and C^2 had a highly significant effect on sensory scores ($P < 0.01$), while primary item A and interaction items AB and BC had a significant effect ($0.01 < P < 0.05$). The *F*-value reflects the degree of influence of each factor on the response value, with larger *F*-values indicating greater influence. Based on the *F* value, it is evident that the primary and secondary factors influencing sensory scores were B, C, and A, respectively, which suggested that CJ had the greatest impact on sensory quality during concoction, followed by GICP and LBJ. The reason might be that carrot contained more volatile composition such as β-ionone, which had a strong sweet and fruity aroma, and golden imperial chrysanthemum contained monoterpenes such as chrysanthenone and 1,8-cineole, which also had lower flavor thresholds, while the flavor substances in *L.barbarum* were mainly non-volatile substances such as betaine and polysaccharides, which had weaker flavor presenting properties, and thus had the least impact on the sensory quality.

Based on the regression equation, a response surface analysis was conducted to examine the interaction of each factor

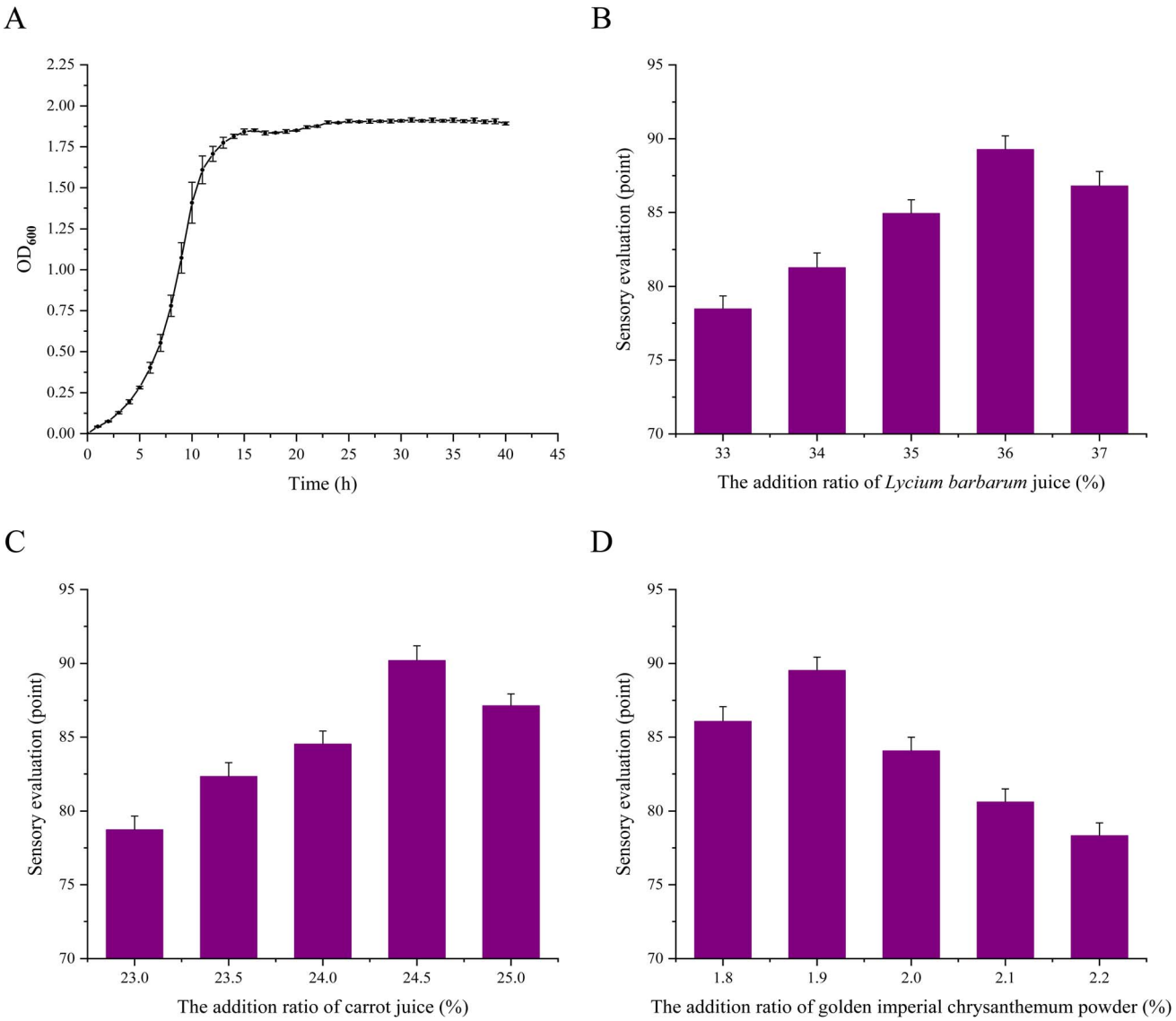

Fig. 1 Analysis of the fermentation concoction process of MEPs. (A) Growth curves of fermentation strains; (B) single-factor test on the addition ratio of *Lycium barbarum* juice; (C) single-factor test on the addition ratio of carrot juice; (D) single-factor test on the addition ratio of golden imperial chrysanthemum powder.

(Fig. 2). The response surface plots for the three interactions (AB, AC, and BC) all showed a downward trend, indicating the presence of a maximum value. Additionally, the contour plots were all elliptical, suggesting that the interaction of various factors had a significant impact on the sensory scores. After analysis, the formulation with the best flavor of FMJ was determined to be 36.16% LBJ, 24.57% CJ, and 1.88% GICP. The predicted sensory score for FMJ under these conditions was 93.1044 points. To ensure the accuracy of the model prediction and the operability of the experiment, the amounts of the three Chinese MEP ingredients were adjusted to 36.2% LBJ, 24.6% CJ, and 1.9% GICP. The test was conducted three times under these conditions, and the final adjusted sensory score of FMJ was 92.97, which closely matched the predicted value. This indicated that the concoction formulation obtained through RSM optimization had practical application value, so the formulation of UFMJ was determined to be 36.2% LBJ, 24.6% CJ, 1.9% GICP, 3% inulin and 34.3% purified water.

After sensory evaluation and response surface analysis, the optimal formulation of the *L.barbarum* herbal mixed juice was determined, and to elucidate the effect of *L.paracasei* 5572 concoction on the medicinal and edible properties of the product and its molecular mechanisms, antioxidant activity and metabolomics assay experiments were also performed.

3.4 Analysis of functional composition and *in vitro* antioxidant activity

Flavonoids are a class of polyphenolic compounds with the structure of benzo-*V*-pyridone, which have strong antioxidant and antiradical effects.[23] Previous studies have shown that flavonoids from fermented foods are more bioavailable than flavonoids from unfermented foods.[24] Based on the standard

Table 2 ANOVA of the regression model for the additions of LBJ, CJ and GICP[a]

Source	Sum of squares	df	Mean square	*F*-value	*P*-value	Significance
Model	46.46	9	5.16	38.53	<0.0001	**
A	0.81	1	0.81	6.02	0.0439	*
B	3.92	1	3.92	29.26	0.0010	**
C	3.05	1	3.05	22.77	0.0020	**
AB	1.61	1	1.61	12.04	0.0104	*
AC	3.61	1	3.61	26.94	0.0013	**
BC	1.28	1	1.28	9.53	0.0176	*
A^2	7.34	1	7.34	54.76	0.0001	**
B^2	10.85	1	10.85	80.95	<0.0001	**
C^2	10.64	1	10.64	79.45	<0.0001	**
Residual	0.94	7	0.13			
Lack of fit	0.58	3	0.18	2.18	0.2326	
Pure error	0.36	4	0.089			
Cor total	47.40	16				
R^2	0.9802					
R^2_{adj}	0.9548					
C.V.%	0.40					
Adeq Precision	18.086					

[a] ** indicates a highly significant difference ($P < 0.01$); * indicates a significant difference ($0.01 < P < 0.05$).

curve of the measured rutin standard ($y = 0.19141x + 0.04975$), the total flavonoid content in UFMJ and FMJ was calculated to be 3.98 ± 0.02 mg mL^{-1} and 4.28 ± 0.05 mg mL^{-1}, respectively, which was an enhancement of about 7.54%. The reason was that flavonoids are secondary metabolites that can be accumulated by probiotic fermentation concoction, and the mechanism involved a group of glycosidases in probiotic bacteria that can release flavonoids and isoflavone aglycones from the corresponding glycosides, which led to an increase in flavonoid content.[25] In addition, flavonoids have strong antioxidant activity, and the increase in their content could help to enhance the antioxidant activity of the MEPs.

Phenolics are also important secondary metabolites in plants and may have good medicinal properties in the treatment of diseases such as diabetes and cancer.[26] Similarly, based on the measured gallic acid standard curve ($y = 5.96321x + 0.06726$), the total phenolics were calculated to be 6.51 ± 0.09 mg mL^{-1} for UFMJ and 9.36 ± 0.09 mg mL^{-1} for FMJ, with a huge enhancement of about 43.79%. This could be attributed to the ability of probiotics to transform phenolic compounds through the action of different glycosyl hydrolases, releasing aglycone from glycol-conjugated phenolic compounds, which led to an increase in phenolic content.[27] In addition, the increased pectinase activity in LBJ after fermentation leads to severe degradation of pectin in the cell wall and subsequent release of polyphenols, given that pectin serves as a carrier for the binding of polyphenols.[28] Furthermore, the content of both phenolics and organic acids such as lactic acid in MEPs increased after fermentation, while the increase in organic acids also hindered the degradation of phenolics. This increase in total phenolic content could augment the ability of MEPs to scavenge free radicals.

Free radicals are atoms or groups with uncoupled electrons that are very active in the human body, attacking normal cells in the body and causing oxidative stress,[29] so the ability to scavenge free radicals is the key to evaluating the antioxidant capacity of foods. As shown in Fig. 3, the scavenging ability of UFMJ, FMJ and Vc for DPPH, ABTS, and ˙OH radicals was illustrated, and the results showed that the scavenging rate of all three radicals increased with the concentration of UFMJ and FMJ and stabilized after reaching a certain value. Moreover, the radical scavenging rate of FMJ was also improved compared to UFMJ. At a concentration of 100 mg mL^{-1}, the DPPH radical scavenging rate increased from $84.56 \pm 1.40\%$ to $91.58 \pm 1.95\%$, the ABTS radical scavenging rate increased from $85.73 \pm 1.40\%$ to $92.05 \pm 1.30\%$, and the ˙OH radical scavenging rate increased from $78.31 \pm 1.66\%$ to $85.67 \pm 1.24\%$, all of which were significantly increased by approximately 7% and close to Vc levels. This is consistent with the previous changes in flavonoids and phenolics, suggesting that probiotic fermentation concoction increased the antioxidant functional composition of MEPs compared to traditional concoction methods.

3.5 Analysis of differential metabolites

The UFMJ was designated as group A and the FMJ as group B. Metabolites in the samples were identified and quantified using UHPLC-MS/MS-based untargeted metabolomics. Metabolites with a *P*-value<0.5 and a VIP-value>1 were considered as differential metabolites. Principal component analysis (PCA), partial least squares-discriminant analysis (PLS-DA), and orthogonal partial least squares-discriminant analysis (OPLS-DA) were performed on the experimental data (Fig. 4A–C). In the OPLS-DA model, $R^2\,x = 0.639$, $R^2\,y = 0.998$, and $Q^2 = 0.967$ were obtained, and the reliability of the model was also verified by a random replacement test with $n = 200$ (Fig. 4D). The results showed that both R^2 and Q^2 decreased. The slope of the Q^2 regression line was greater than 1, and the intercept was less than 0, suggesting that the model was not overfitted and had good predictability. This enabled the screening and analysis of differential metabolites in the composite LBJ before and after fermentation concoction.

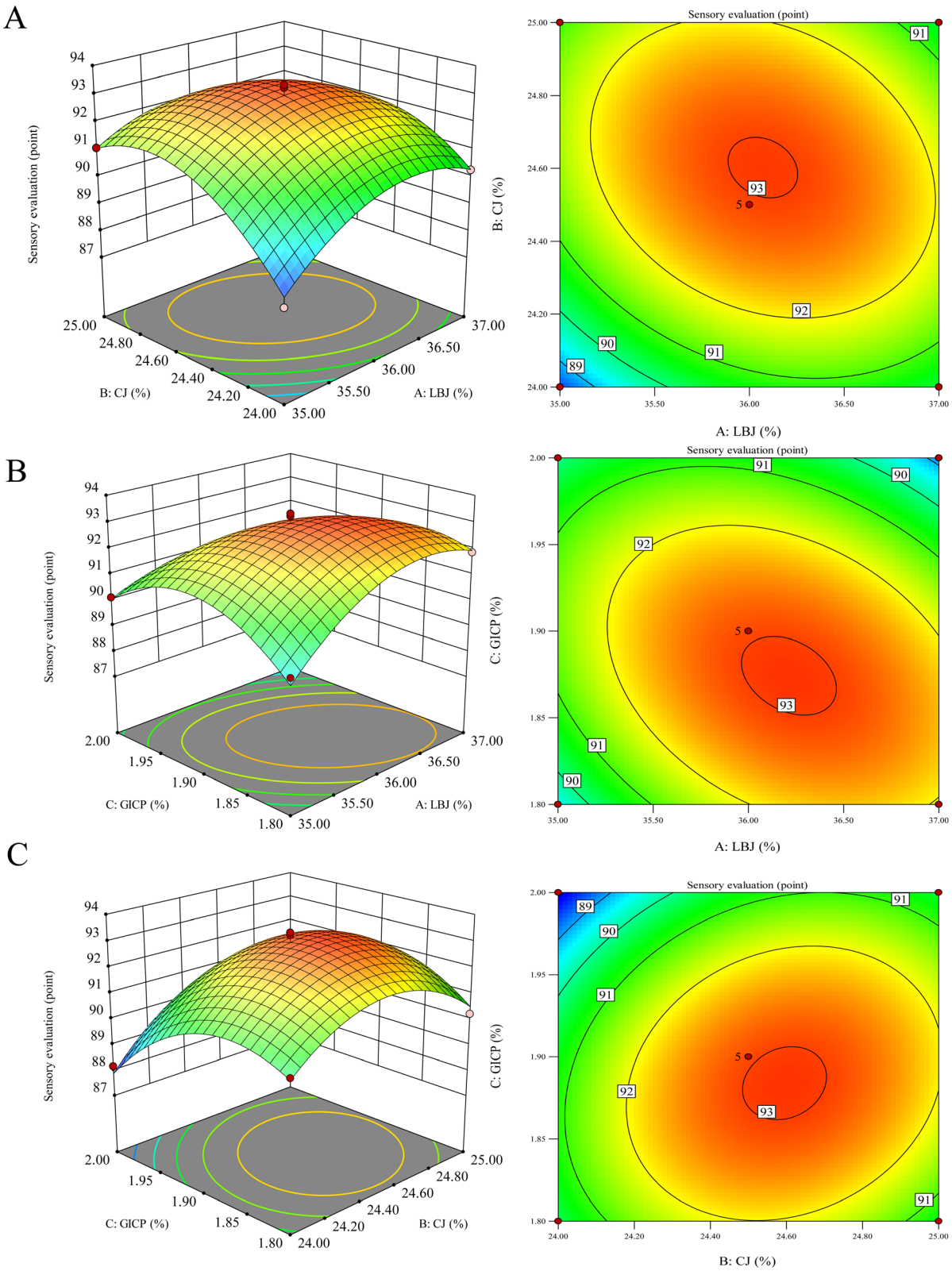

Fig. 2 Response surface analysis of the interaction of the addition ratio of the main raw materials for fermentation. (A) Interaction of LBJ with CJ; (B) interaction of LBJ with GICP; (C) interaction of CJ with GICP.

In addition, a total of 657 differential metabolites from 20 classes in UFMJ and FMJ were screened, such as 130 organic acids and derivatives, 115 phenylpropanoids and polyketides, 114 lipids and lipid-like molecules, 107 organoheterocyclic compounds, 57 organic oxygen compounds, 50 benzenoids, 20 nucleosides, nucleotides, and analogues, 12 alkaloids and

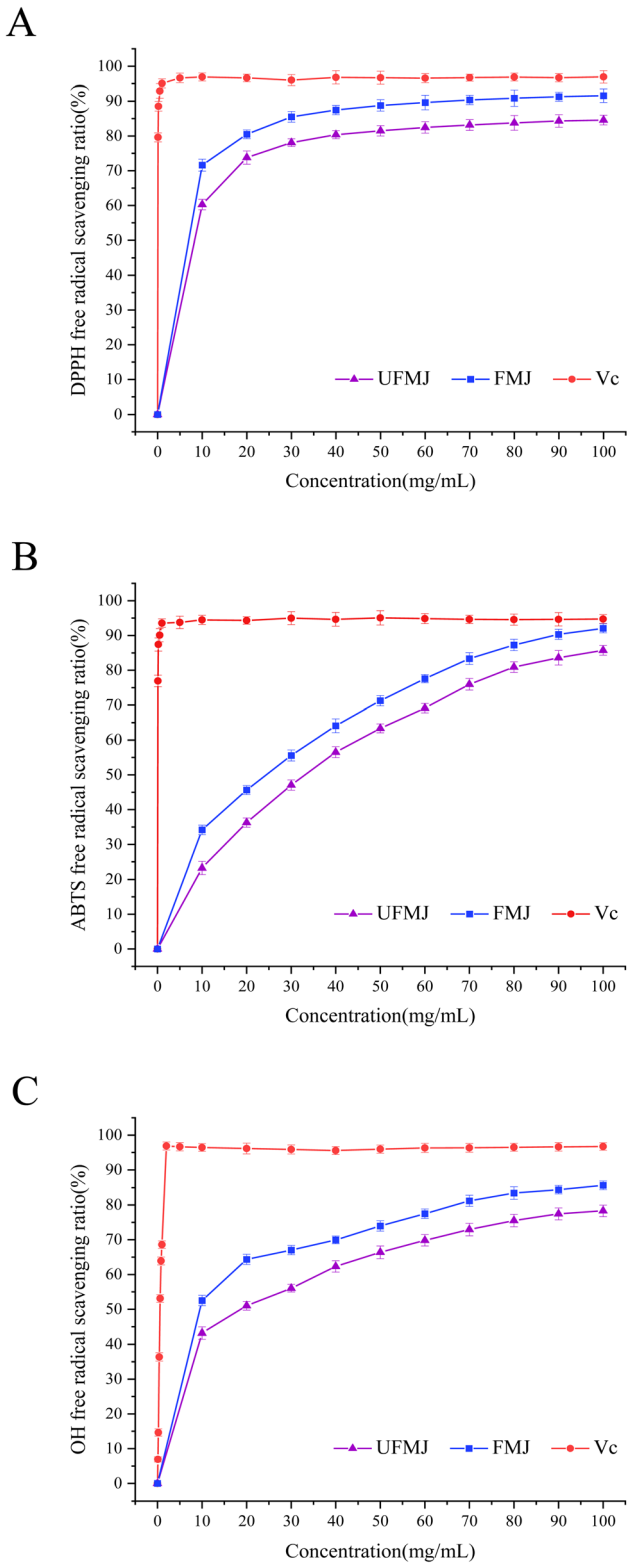

Fig. 3 Free radical scavenging curves of UFMJ, FMJ and Vc. (A) DPPH radical scavenging curves; (B) ABTS radical scavenging curves; (C)˙OH radical scavenging curves.

derivatives, 6 lignans, neolignans and related compounds, 6 organic nitrogen compounds, 4 benzene and substituted derivatives, 2 hydrocarbon derivatives, *etc.*, of which 242 metabolites were up-regulated and 415 metabolites were down-regulated, and volcano diagrams were plotted for the visualization and analysis, as shown in Fig. 4E.

To more comprehensively and intuitively represent the relationship between samples and the differences in metabolite expression patterns in different samples, a differential metabolite clustering heatmap was plotted (Fig. 5A), and the differential metabolites with the top 50 VIP values were also labeled (Fig. 5B). As can be seen from Fig. 5B, the metabolites that were significantly up-regulated in FMJ samples compared to UFMJ samples were mainly dipeptides and nucleosides, where the *C*-terminus in the dipeptides was mainly proline, a structure that has some anti-hypertensive health benefits[30] and proline is also a strong antioxidant, and its content is positively correlated with the scavenging rate of DPPH and ABTS free radicals.[31] Among the *N*-terminal amino acids in the dipeptide, the most abundant were pyroglutamic acid, aspartic acid and histidine, and pyroglutamic acid promotes the survival of ganglion cells in the retina,[32] which is of greater benefit to the eyes, and aspartic acid is a fresh flavored amino acid[33] that adds freshness to the beverage, while histidine plays an important role in anti-inflammatory and antioxidant processes, and treatment of a variety of diseases.[34] In addition, among the significantly up-regulated nucleoside metabolites, there were hypoxanthine, inosine, 6-*n*-propyl uracil and 2,3-dideoxyuridine, *etc.* Among them, hypoxanthine can promote the development of human intellect and the absorption of iron in appropriate amounts and also improve the flavor of food;[35] inosine, which is formed by the combination of hypoxanthine and ribose, not only enhances the flavor of food,[36] but also has a strong immunomodulatory and neuroprotective effect,[37] can significantly increase the axonal regeneration of retinal ganglion cells;[38] uracil and uridine are also similar substances; uracil combined with ribose can form uridine. Uridine has the ability to slow down the aging of the body's stem cells and increase the efficacy of antioxidant enzymes[39] and it is hypothesized that this substance contributes to the increase in the antioxidant activity of MEPs. For the metabolites that were significantly down-regulated in the FMJ samples, the main ones were dipeptides composed of leucine, isoleucine and phenylalanine, which are bitter amino acids,[40,41] and the reduction of the content of the dipeptides composed of them was able to improve the flavor of the beverages and make them more acceptable. Also, after fermentation concoction by *L.paracasei* 5572, a significant decrease in malic acid content occurred, probably due to the conversion of malic acid into other beneficial substances such as lactic acid by probiotics through the TCA cycle or malolactic fermentation.[42] These suggested that probiotic fermentation as a novel concoction method of MEPs had the characteristics of toxicity reduction, flavor correction and potency enhancement.

3.6 Analysis of KEGG pathway enrichment

The fermentation concoction of probiotics is a complex metabolic operation that necessitates the coordinated regulation of various physiological and biochemical reactions. Consequently, it is imperative to delve deeper into its metabolic pathways. The

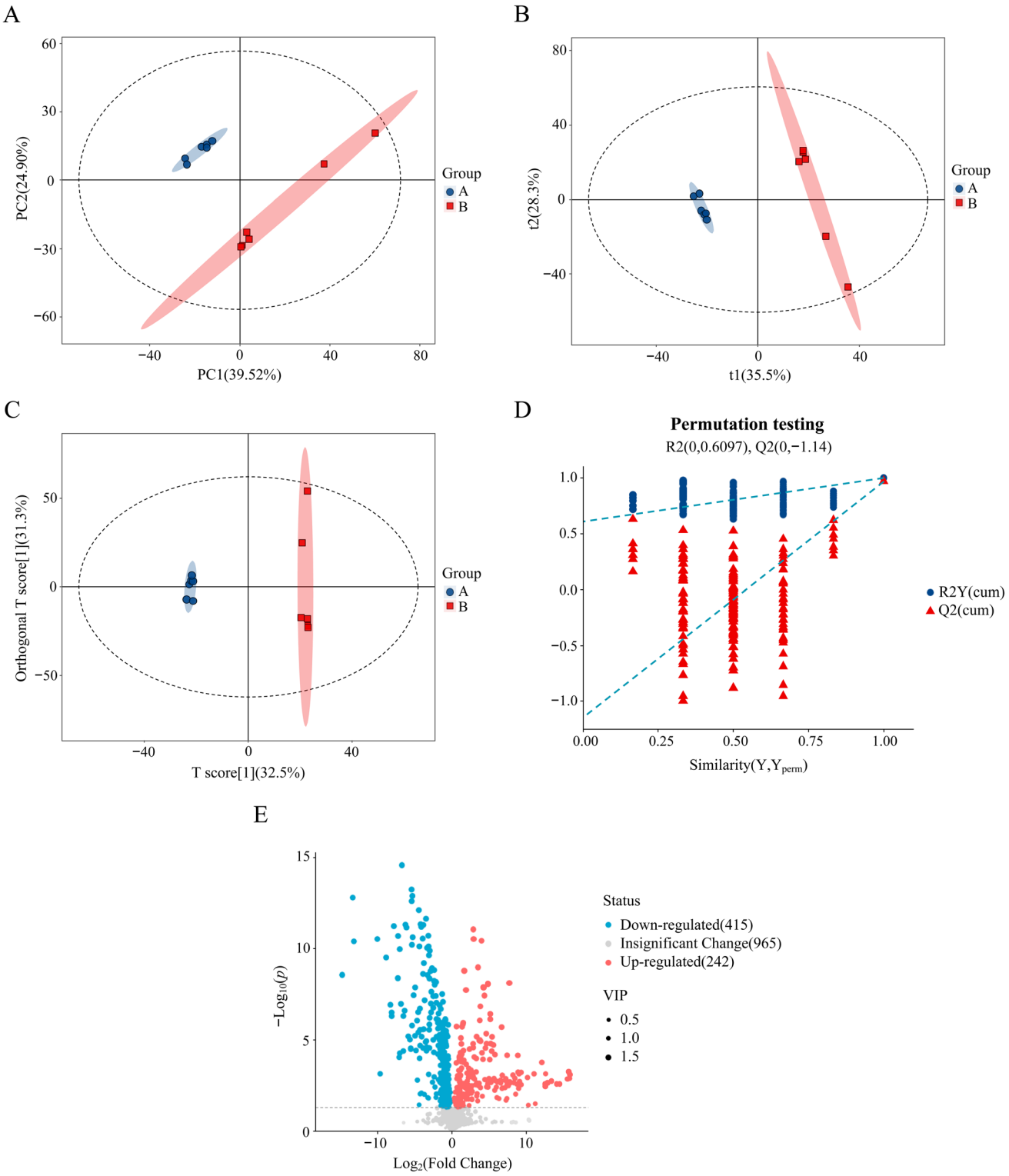

Fig. 4 Screening and comparative analysis of differential metabolites. (A) PCA score plot; (B) PLS-DA score plot; (C) OPLS-DA score plot; (D) OPLS-DA replacement test plot; (E) FMJ *vs.* UFMJ differential metabolite volcano plot.

KEGG database was used to match differential metabolites identified from UFMJ and FMJ with their corresponding pathways to obtain pathway information related to these metabolites. Enrichment analysis was conducted on the annotation results to determine the pathways for significant enrichment of differential metabolites. The findings revealed that a total of 30 significant metabolic pathways involved differential metabolites in UFMJ and FMJ were identified. As illustrated in Fig. 6A,

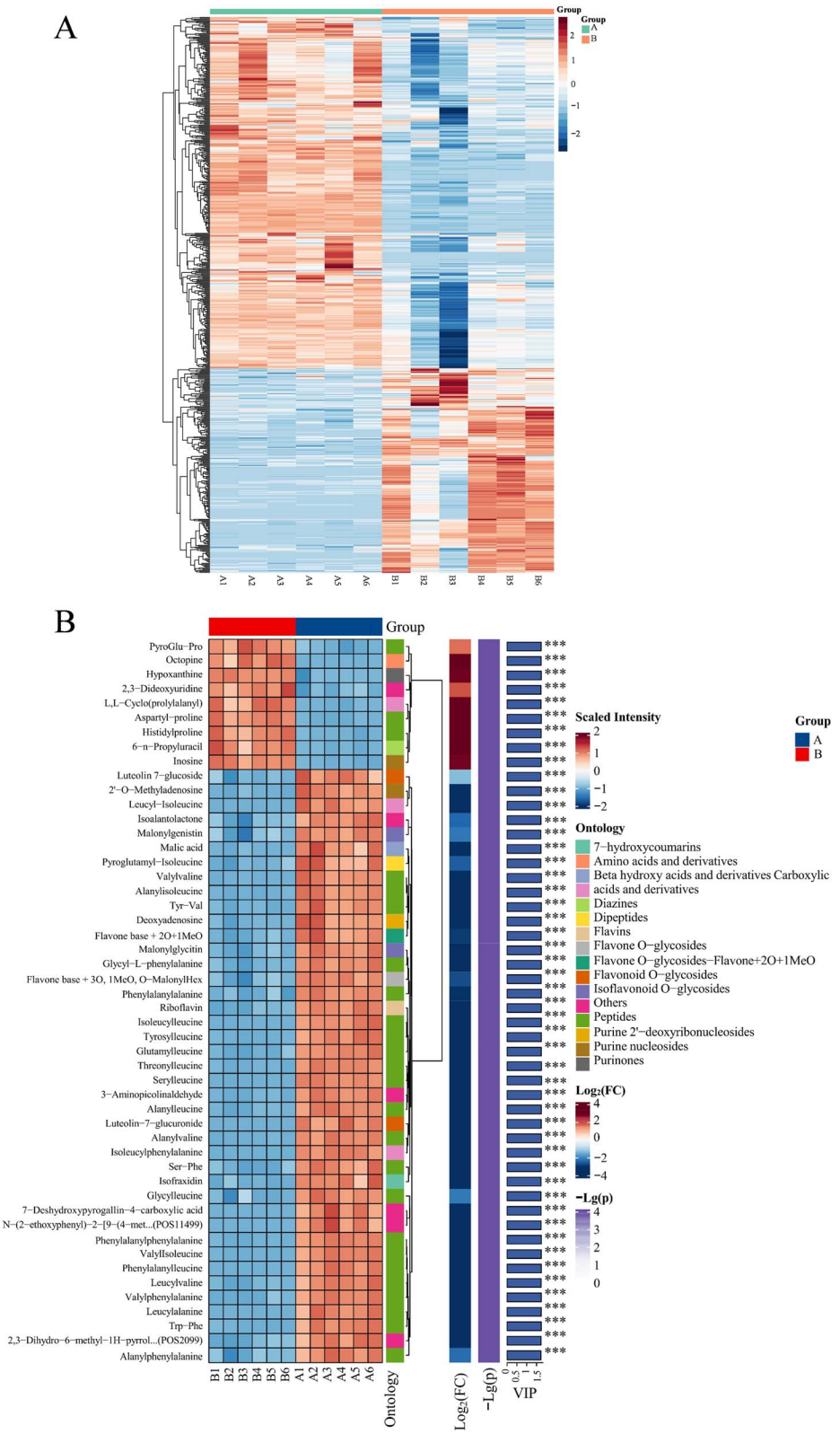

Fig. 5 Hierarchical cluster analysis of differential metabolites. (A) Simple heat map of differential metabolites of samples before and after fermentation concoction; (B) complex heat map of differential metabolites of samples before and after fermentation concoction. The redder color indicates higher relative expression and the bluer color indicates lower relative expression.

during the fermentation concoction of UFMJ into FMJ by *L.paracasei* 5572, both synthesis and degradation pathways are implicated, and the metabolic pathways, ATP binding cassette (ABC) transporters, biosynthesis of flavonoids and flavonols, biosynthesis of flavones, and purine metabolism were primarily enriched. Notably, metabolic pathways, ABC transporters, and

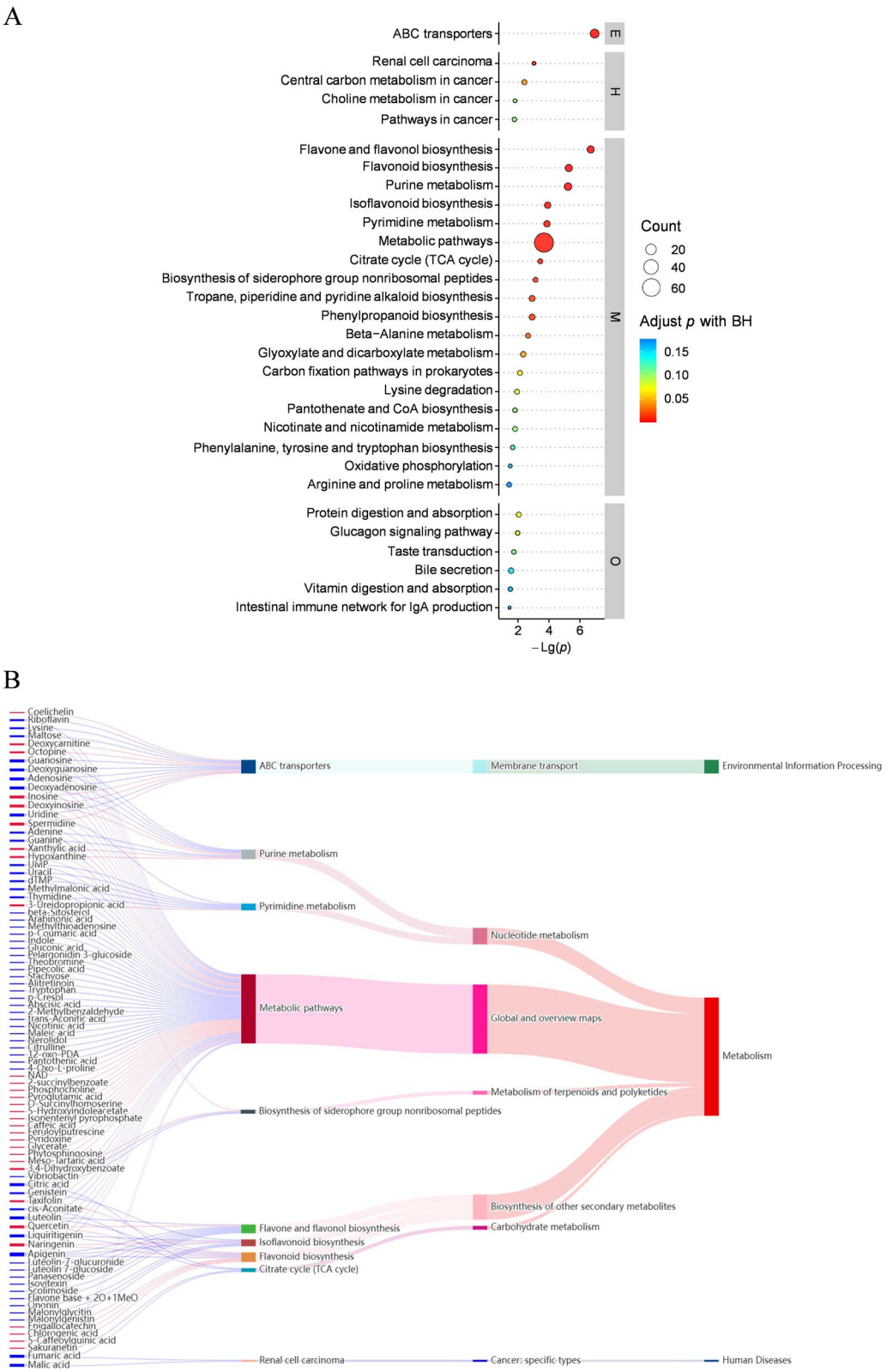

Fig. 6 KEGG metabolic pathway analysis. (A) KEGG metabolic pathway enrichment bubble diagram; (B) KEGG metabolic pathway Sankey diagram.

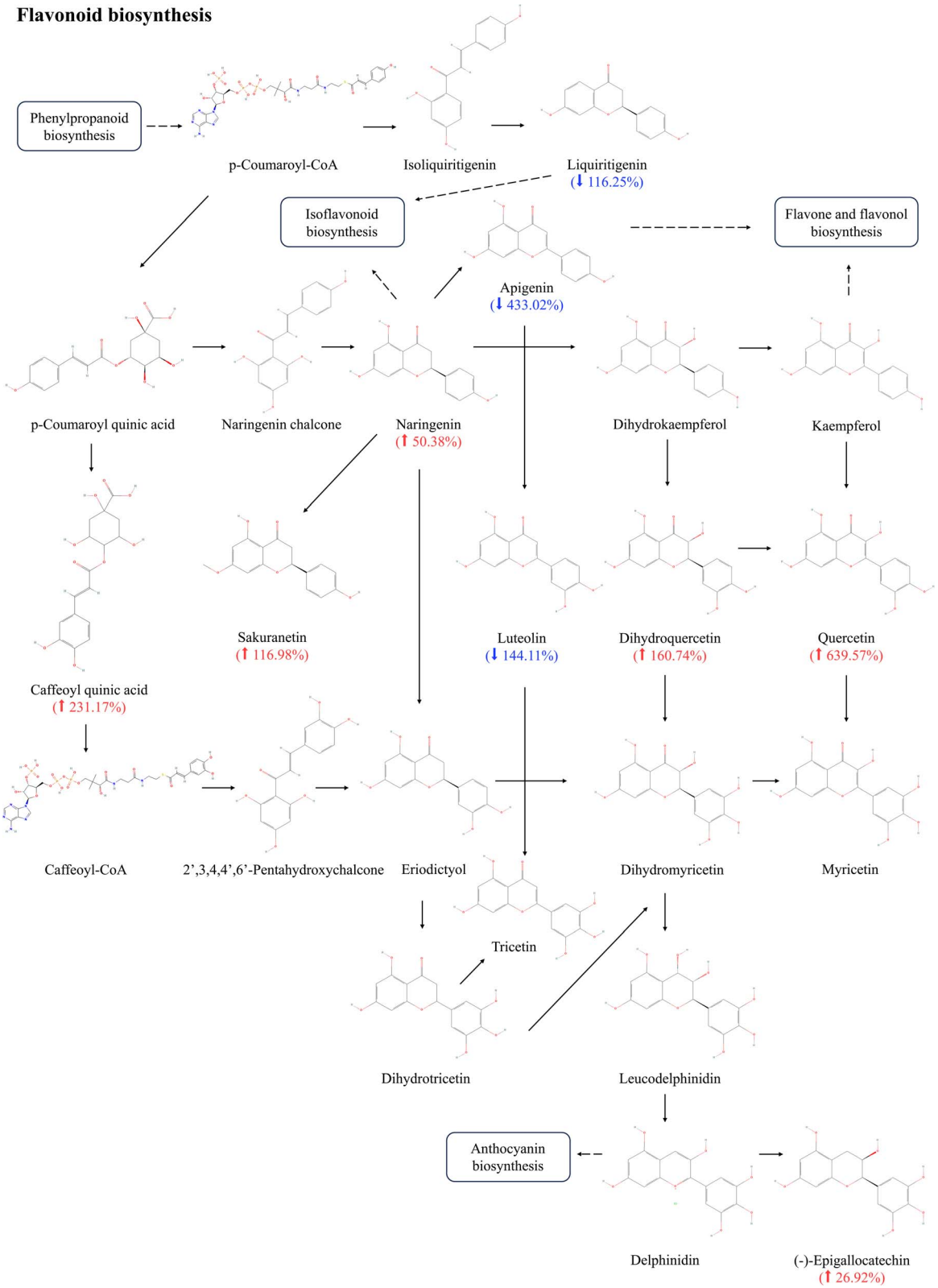

Fig. 7 Analysis of the flavonoid biosynthesis metabolic pathway. Red font represents significantly up-regulated metabolites, blue font represents significantly down-regulated metabolites, solid lines represent transformations between metabolites and dashed lines represent other metabolic pathways involved in the metabolite.

purine metabolism played a crucial role in ensuring the growth and development of microorganisms and enhancing the flavor and functional substances in beverages. Furthermore, the enrichment of biosynthesis of flavonoids and flavonols and biosynthesis of flavones suggested that fermentation concoction generated a large amount of flavonoid substances, which might be the main reason for the increased antioxidant activity of MEPs.

To elucidate the interplay between metabolites and metabolic pathways, a Sankey diagram was plotted to depict the data flow of up-regulated and down-regulated metabolites in UFMJ and FMJ samples across various KEGG pathway levels (Fig. 6B). The leftmost column of the figure delineates significantly different metabolites, and the subsequent columns represent increasing levels of metabolic pathways. As illustrated, for metabolites associated with the TCA cycle, FMJ exhibited a declining trend relative to UFMJ, indicating that metabolites participating in TCA cycle reactions such as citric acid and *cis*-aconitate were consumed by *L.paracasei* 5572, providing a material basis for the strain's secondary metabolism, which was consistent with the natural laws of microbial metabolism. Furthermore, metabolites that may be associated with renal cell carcinoma, such as fumaric acid and malic acid, were also significantly reduced in FMJ compared to UFMJ. This implied that oxidative phosphorylation rates in tumor cells might diminish.[43] The above findings demonstrated the probiotic potential of *L.paracasei* 5572 during fermentation concoction, significantly reducing the metabolites of MEPs that may induce human diseases. Most importantly, for metabolites involved in the flavonoid biosynthesis pathway, such as quercetin, naringenin, epicatechin and chlorogenic acid with strong antioxidant activity, the FMJ showed an increasing trend compared to the UFMJ, indicating that the metabolites producing flavonoids were significantly increased after fermentation concoction by *L.paracasei* 5572. This facilitated the increase of flavonoid content in MEPs, suggesting that the concoction method of probiotic fermentation played an important role in improving the antioxidant activity of MEPs.

To further elucidate the molecular mechanisms by which flavonoids affected the antioxidant activity of MEPs during fermentation concoction, their KEGG metabolic pathway and the differential metabolites therein were analyzed. As illustrated in Fig. 7, the conversion of *p*-coumaroyl-CoA to *p*-coumaroyl quinic acid and naringenin chalcone was facilitated by *L.paracasei* 5572 fermentation concoction. This process increased the production of caffeoyl quinic acid and naringenin, which are thought to be precursors for subsequent reactions, and the increase in the yield of subsequent products such as sakuranetin, dihydroquercetin, quercetin, and (−)-epigallocatechin was also facilitated by the increase in these two precursors. Notably, the content of quercetin showed the most significant increase, which was boosted by about 639.57% after fermentation. All of the above substances are flavonoids with potent antioxidant activity, and their significant increase was intrinsically linked to the enhancement in total flavonoid content and antioxidant activity of MEPs after fermentation concoction.

4 Conclusion

Based on the above results, the biotransformation of probiotic fermentation concoction had a positive effect on the sensory quality and functional composition of Chinese MEPs. For formulation optimization, the concoction formulation of the product with the best sensory quality was determined by RSM optimization. For functional composition and antioxidant activity, the contents of total flavonoids and total phenolics as well as the scavenging rate of three free radicals (DPPH, ABTS, and ˙OH) in the product were all increased after *L.paracasei* 5572 fermentation concoction. For metabolomics, the molecular mechanism of the increased sensory quality and functional composition after *L.paracasei* 5572 fermentation concoction involved significant increases in dipeptides, nucleosides and flavonoids in the products. Furthermore, the product might have a positive effect on eye protection due to increased antioxidant activity and eye-healthy substances. In conclusion, this study described a novel method for pairing and concoction of Chinese MEPs and explored their effects and mechanisms, providing a theoretical basis for future development of probiotic fermentation of more plants.

Informed consent statement

All participants in this sensory evaluation were voluntarily enrolled and had signed the relevant informed consent in advance. The informed consent protects the rights and privacy of all participants. For example, it was guaranteed that all assessment data were collected and used with the knowledge and consent of the participants, the confidentiality of the participants' personal information was guaranteed and they were informed in advance of the requirements and risks of the study, as well as the right to withdraw from the evaluation at any time without having to give a reason.

Abbreviations

MEP	Medicinal and Edible Plant
NFC	Not From Concentrate
UFMJ	Unfermented *Lycium barbarum* Herbal Mixed Juice
FMJ	Fermented *Lycium barbarum* Herbal Mixed Juice
LBJ	*Lycium barbarum* Juice
CJ	Carrot Juice
GICP	Golden Imperial Chrysanthemum Powder
DPPH	2,2-diphenyl-1-picrylhydrazyl
ABTS	2,2′-Azinobis-(3-ethylbenzthiazoline-6-sulphonate)
LC-MS	Liquid Chromatograph-Mass Spectrometer
RSM	Response Surface Methodology
BBD	Box–Behnken Design
VIP	Variable Importance in Projection
PCA	Principal Component Analysis
PLS-DA	Partial Least Squares Discriminant Analysis
OPLS-DA	Orthogonal Partial Least Squares Discriminant Analysis

Ethical statement

This sensory evaluation was approved by our institution's Science and Technology Ethics Committee for ethical permission to conduct a human sensory evaluation study (Approval No. NXU-H-2023-160). In addition, the products for this sensory evaluation were beverages within the food category, and their quality had been tested and complied with the National Standards of the People's Republic of China (Standard No. GB 7101-2022) before the sensory evaluation to ensure that they were safe to drink.

Data availability

The data supporting this article have been included as part of the ESI.†

Author contributions

Zhengxu An: conceptualization, methodology, investigation, formal analysis, data curation, and writing – original draft. Tong Ye: methodology, software, formal analysis, visualization, and writing – original draft. Junwei Yu: resources and methodology. Hongjun Wu: resources. Peirong Niu: methodology and investigation. Xiaobo Wei: software and visualization. Huiyan Liu: resources, validation, project administration, formal analysis, and funding acquisition. Haitian Fang: conceptualization, methodology, writing – review & editing, validation, supervision, project administration, and funding acquisition.

Conflicts of interest

The authors declare that they have no known competing financial interests or personal relationships that could have appeared to influence the work reported in this paper.

Acknowledgements

This work was supported by The Key Research and Development Program of Ningxia [grant number 2024ZDYF0480]; The Ningxia Hui Autonomous Region Youth Top Talent Training Project [grant number 022004000010]; The Helanshan Scholars Program of Ningxia University [grant number No. 2020]; The Innovative Project of Ningxia University Goji Modern Industry school [grant number No. 2023]. We also thank Shanghai Bioprofile Technology Company Ltd. for technological assistance in untargeted metabolomics experiment.

References

1 A. S. Chopra, R. Lordan, O. K. Horbańczuk, A. G. Atanasov, I. Chopra, J. O. Horbańczuk, A. Jóźwik, L. Huang, V. Pirgozliev, M. Banach, M. Battino and N. Arkells, *Pharmacol. Res.*, 2022, **175**, 106001.
2 J. Bi, H. Fang, J. Zhang, L. Lu, X. Gu and Y. Zheng, *J. Future Foods*, 2023, **3**, 240–251.
3 W. Duan, L. Zhou, Y. Ren, F. Liu, Y. Xue, F.-Z. Wang, R. Lu, X.-J. Zhang, J.-S. Shi, Z.-H. Xu and Y. Geng, *Food Funct.*, 2024, **15**, 1612–1626.
4 S. Motegaonkar, A. Shankar, H. Tazeen, M. Gunjal and S. Payyanad, *Sustainable Food Technol.*, 2024, **2**, 667–688.
5 C. Li, S.-P. Nie, K.-X. Zhu, T. Xiong and M.-Y. Xie, *Food Res. Int.*, 2016, **80**, 36–40.
6 S.-J. Zhu, S.-H. He, W.-J. Miao, X. Sun, C.-H. Shi, D. Liu and L. Yang, *Curr. Top. Nutraceutical Res.*, 2021, **19**, 157–164.
7 V. E. Vera-Santander, E. Mani-López, A. López-Malo and M. T. Jiménez-Munguía, *Sustainable Food Technol.*, 2024, **2**, 1101–1112.
8 W. Akram, V. Pandey, R. Sharma, R. Joshi, N. Mishra, N. Garud and T. Haider, *Int. J. Biol. Macromol.*, 2024, **259**, 129131.
9 N. Liu, L. Qin, M. Mazhar and S. Miao, *J. Proteomics*, 2021, **238**, 104158.
10 J. Yang, C. Dong, F. Ren, Y. Xie, H. Liu, H. Zhang and J. Jin, *J. Sci. Food Agric.*, 2022, **102**, 3107–3118.
11 M. Marnpae, C. Chusak, V. Balmori, K. Kamonsuwan, W. Dahlan, T. Nhujak, N. Hamid and S. Adisakwattana, *LWT–Food Sci. Technol.*, 2022, **169**, 113986.
12 L. C. Midlej, S. F. Arruda, M. C. Mesquita, M. A. Mendonça and E. dos Santos Leandro, *J. Funct.Foods*, 2023, **111**, 105883.
13 X. Chen, Z. Zhu, X. Zhang, L. Chen, Q. Gu and P. Li, *J. Dairy Sci.*, 2024, **107**(8), 5280–5300.
14 H. Xie, P. Gao, Z.-M. Lu, F.-Z. Wang, L.-J. Chai, J.-S. Shi, H.-L. Zhang, Y. Geng, X.-J. Zhang and Z.-H. Xu, *Food Biosci.*, 2023, **54**, 102881.
15 X. Chen, X. Jia, S. Yang, G. Zhang, A. Li, P. Du, L. Liu and C. Li, *LWT–Food Sci. Technol.*, 2022, **165**, 113725.
16 P.-H. Huang, C.-S. Chiu, Y.-J. Chan, S.-J. Chen, W.-C. Lu and P.-H. Li, *J. Agric. Food Res.*, 2023, **14**, 100855.
17 J. Zhishen, T. Mengcheng and W. Jianming, *Food Chem.*, 1999, **64**, 555–559.
18 V. L. Singleton and J. A. Rossi, *Am. J. Enol. Vitic.*, 1965, **16**, 144–158.
19 X. Yang, S. Yang, Y. Guo, Y. Jiao and Y. Zhao, *Food Chem.*, 2013, **138**, 1256–1264.
20 S. J. Padayatty, A. Katz, Y. Wang, P. Eck, O. Kwon, J.-H. Lee, S. Chen, C. Corpe, A. Dutta, S. K. Dutta and M. Levine, *J. Am. Coll. Nutr.*, 2003, **22**, 18–35.
21 J.-J. Wang, W.-W. Zhang, Z.-J. Guan, K. Thakur, F. Hu, J.-G. Zhang and Z.-J. Wei, *Food Chem.*, 2023, **409**, 135277.
22 N. Smirnoff and Q. J. Cumbes, *Phytochemistry*, 1989, **28**, 1057–1060.
23 S. Kumar and A. K. Pandey, *Sci. World J.*, 2013, **2013**, 1–16.
24 R. Di Cagno, F. Mazzacane, C. G. Rizzello, O. Vincentini, M. Silano, G. Giuliani, M. De Angelis and M. Gobbetti, *J. Agric. Food Chem.*, 2010, **58**, 10338–10346.
25 R. Tang, Y. Qin and Y. Luo, *Int. J. Food Microbiol.*, 2025, **427**, 110974.
26 C. Guan, X. Zhou, H. Li, X. Ma and J. Zhuang, *Biomed. Pharmacother.*, 2022, **156**, 113951.
27 B. B. T. De Assis, T. C. Pimentel, A. M. Dantas, M. Dos Santos Lima, G. Da Silva Campelo Borges and M. Magnani, *Food Res. Int.*, 2021, **146**, 110435.

28 S. Liu, Y. He, W. He, X. Song, Y. Peng, X. Hu, S. Bian, Y. Li, S. Nie, J. Yin and M. Xie, *J. Agric. Food Chem.*, 2024, **72**, 12752–12761.
29 Y. Liu, Z. Wang, H. Li, M. Liang and L. Yang, *J. Sci. Food Agric.*, 2016, **96**, 4940–4950.
30 B. F. Gibbs, A. Zougman, R. Masse and C. Mulligan, *Food Res. Int.*, 2004, **37**, 123–131.
31 A. Laophongphit, S. Siripornadulsil and W. Siripornadulsil, *LWT–Food Sci. Technol.*, 2023, **181**, 114756.
32 S. Oono, T. Kurimoto, T. Nakazawa, T. Miyoshi, N. Okamoto, R. Kashimoto, Y. Tagami, Y. Ito and O. Mimura, *Curr. Eye Res.*, 2009, **34**, 598–605.
33 X. Li, S. Chen, K.-H. Ouyang and W.-J. Wang, *Res. Vet. Sci.*, 2022, **149**, 11–20.
34 A. E. Thalacker-Mercer and M. E. Gheller, *J. Nutr.*, 2020, **150**, 2588S–2592S.
35 S. Ichimura, Y. Nakamura, Y. Yoshida and A. Hattori, *Anim. Sci. J.*, 2017, **88**, 379–385.
36 H. Li, G. Zhang, A. Deng, N. Chen and T. Wen, *Biotechnol. Lett.*, 2011, **33**, 1575–1580.
37 G. Haskó, M. V. Sitkovsky and C. Szabó, *Trends Pharmacol. Sci.*, 2004, **25**, 152–157.
38 M.-M. Wu, S.-W. You, B. Hou, X.-Y. Jiao, Y.-Y. Li and G. Ju, *Neurosci. Lett.*, 2003, **341**, 84–86.
39 J. Ye, Z. Jin, S. Chen and W. Guo, *Cell Cycle*, 2022, **21**, 33–48.
40 T. Wang, L. Li, Y. Cong, S. Gao, Z. Wu and W. Sun, *J. Food Compos. Anal.*, 2023, **121**, 105408.
41 J. Yang, D.-S. Waterhouse and C. Cui, *Encycl. Food Chem.*, 2019, 505–509.
42 W. Duan, Q. Guan, H.-L. Zhang, F.-Z. Wang, R. Lu, D.-M. Li, Y. Geng and Z.-H. Xu, *Food Chem.*, 2023, **408**, 135155.
43 A. A. Hakimi, E. Reznik, C.-H. Lee, C. J. Creighton, A. R. Brannon, A. Luna, B. A. Aksoy, E. M. Liu, R. Shen, W. Lee, Y. Chen, S. M. Stirdivant, P. Russo, Y.-B. Chen, S. K. Tickoo, V. E. Reuter, E. H. Cheng, C. Sander and J. J. Hsieh, *Cancer Cell*, 2016, **29**, 104–116.